



Research paper

# Novel in-capsule synthesis of metal–organic framework for innovative carbon dioxide capture system

Wei Yu <sup>a,b</sup>, Ming Gao <sup>b,c</sup>, Guanhe Rim <sup>b,c,d</sup>, Tony G. Feric <sup>b,d</sup>, Mark L. Rivers <sup>e</sup>, Ammar Alahmed <sup>f</sup>,  
Aqil Jamal <sup>f</sup>, Ah-Hyung Alissa Park <sup>b,c,d,\*</sup>

<sup>a</sup> State Key Laboratory of Clean Energy Utilization, Zhejiang University, Hangzhou, 310027, China

<sup>b</sup> Lenfest Center for Sustainable Energy, The Earth Institute, Columbia University, 918 S.W. Mudd Hall, Mail Code 4711, 500 W 120<sup>th</sup> St., New York, NY, 10027, USA

<sup>c</sup> Department of Earth and Environmental Engineering, Columbia University, 918 S.W. Mudd Hall, Mail Code 4711, 500 W 120<sup>th</sup> St., New York, NY, 10027, USA

<sup>d</sup> Department of Chemical Engineering, Columbia University, New York, NY, 10027, USA

<sup>e</sup> University of Chicago, Chicago, IL, 60637, USA

<sup>f</sup> Research and Development Center, Saudi Aramco, Dhahran, 31311, Saudi Arabia

Received 29 June 2021; revised 16 August 2021; accepted 20 August 2021

Available online 24 August 2021

## Abstract

Metal–Organic Frameworks (MOFs) have been developed as solid sorbents for CO<sub>2</sub> capture applications and their properties can be controlled by tuning the chemical blocks of their crystalline units. A number of MOFs (e.g., HKUST-1) have been developed but the question remains how to deploy them for gas–solid contact. Unfortunately, the direct use of MOFs as nanocrystals would lead to serious problems and risks. Here, for the first time, we report a novel MOF-based hybrid sorbent that is produced via an innovative in-situ microencapsulated synthesis. Using a custom-made double capillary microfluidic assembly, double emulsions of the MOF precursor solutions and UV-curable silicone shell fluid are produced. Subsequently, HKUST-1 MOF is successfully synthesized within the droplets enclosed in the gas permeable microcapsules. The developed MOF-bearing microcapsules uniquely allow the deployment of functional nanocrystals without the challenge of handling ultrafine particles, and further, can selectively reject undesired compounds to protect encapsulated MOFs.

© 2021 Institute of Process Engineering, Chinese Academy of Sciences. Publishing services by Elsevier B.V. on behalf of KeAi Communications Co., Ltd. This is an open access article under the CC BY-NC-ND license (<http://creativecommons.org/licenses/by-nc-nd/4.0/>).

**Keywords:** Encapsulation; Metal–Organic Frameworks (MOFs); Carbon capture; In-situ microencapsulated synthesis

## 1. Introduction

The use of fossil fuels, including coal and natural gas, in power generation will continue while we make a transition to renewable electricity. One of the most difficult challenges associated with fossil fuel-based power is carbon emissions

having a tremendous environmental impact including climate change. Thus, there are serious global efforts to develop effective carbon capture, utilization, and storage (CCUS) technologies. Unfortunately, the enormous scale of the problem prevents their rapid large-scale deployments. Thus, several efforts are being pursued to provide an array of solutions while advancing science [1–5].

Amine scrubbing is one of the widely developed methods for CO<sub>2</sub> capture using liquid solvent [6] and a number of large-scale demonstrations are ongoing (e.g., the Boundary Dam project in Canada and the Petra Nova project in the USA) [4].

\* Corresponding author. Lenfest Center for Sustainable Energy, The Earth Institute, Columbia University, USA.

E-mail address: [ap2622@columbia.edu](mailto:ap2622@columbia.edu) (A.-H. Alissa Park).

Other materials such as solid sorbents have also been proposed to reduce the energy consumption and equipment investment costs of carbon capture technologies [7–9]. These CO<sub>2</sub> adsorption materials, such as activated carbon and zeolites, are limited by their carbon capture capacities. Therefore, there is an increasing interest in developing advanced materials, such as nanomaterial adsorbents, for better CO<sub>2</sub> capture. Metal–Organic Frameworks (MOFs) are porous crystalline materials consisting of metal ions or clusters acting as connecting nodes, and organic ligands acting as linkers [10]. Due to their uniquely controlled structures and great gas sorption capacity, MOFs have exhibited specialized functionality for capturing different molecules and have been one of the most studied materials in recent years [11,12]. Their applications range from gas separation (e.g., CO<sub>2</sub> capture), gas storage (e.g., methane), drug delivery, semiconductors, desalination, and ion separation, etc. [13–15].

While MOFs have many positive properties including high capture capacity and good selectivity in terms of CO<sub>2</sub> capture [16,17], the synthesis of MOFs via hydrothermal or solvothermal methods is time-consuming, which will usually take several hours or days to form the nanoporous network of these crystals. Microwave or ultrasound-assisted synthesis can accelerate the crystallization of MOFs significantly, but will involve additional equipment which may lead to higher energy consumption. Additionally, the scale of MOF synthesis is typically limited. Another important question that has not been answered yet is how to deploy MOFs in a CO<sub>2</sub> capture system. The synthesized MOFs are in the form of nanoparticles or their agglomerates. Thus, the direct use of these fine particles in CO<sub>2</sub> capture devices would lead to many operational problems (e.g., high-pressure drops) and environmental risks (e.g., emission of fine particulates). A few methods have been suggested to allow an easier delivery of MOFs, such as grafting MOFs onto other adsorbents larger in size (e.g. polymer and zeolite), turning MOF particles into granules, pellets, and thin films, and incorporating MOFs in a membrane system [18]. Most of these methods start with already produced MOF crystals and the placement of MOFs is often at the outer layer of the hybrid system, which compromises the CO<sub>2</sub> sorption capacity per mass of adsorbent.

We recently developed the microencapsulation for delivering CO<sub>2</sub> capture materials [19]. This approach is designed to provide enhanced mass transfer for water-lean CO<sub>2</sub> capture solvents such as ionic liquids and Nanoparticle Organic Hybrid Material (NOHMs) [20]. The microencapsulation of viscous solvents in a highly gas-permeable shell is capable of facilitating a faster CO<sub>2</sub> capture, as well as easy handling of the viscous solvents [21–28]. This research inspired us to create a whole new approach to synthesizing and delivering MOFs. If MOF precursor solutions can be encapsulated and MOFs can be directly synthesized within the microcapsules, the size of MOFs can be kept small (i.e., nanocrystals) allowing minimum defects and maximum interfacial area for CO<sub>2</sub> capture. The gas-permeable shell would allow for a

flexible design of CO<sub>2</sub> capture devices and may also provide additional protection for MOFs from moisture and fine particles, etc. Further, the synthesis of MOFs inside microliter droplets has been reported to largely shorten the synthesis time from hours/days to several minutes, as a result of highly efficient mixing and heat transfer [29].

This study focuses on a novel MOF-based hybrid sorbent that is for the first time produced via an innovative in-situ encapsulated synthesis with glass double-capillary devices. For this purpose, the synthesis of a representative MOF structure of HKUST-1 was demonstrated via this method. The developed MOF-bearing microcapsules were characterized by various tools and tested for CO<sub>2</sub> capture.

## 2. Material and methods

### 2.1. Encapsulation and MOF synthesis using a microfluidic device

Encapsulated MOFs are produced using a double-capillary device, which consists of an outer square tube (CAT# 8290-100, VitroCom, Mountain Lakes, NJ) and two inner round tubes (CAT# CV7087-B-100, Mountain Lakes, NJ), one of which is drawn down to a fine tip using a laser tip puller (P-2000 Tip Puller, Sutter Instruments, Novato, CA) and cut to a diameter of 100–150 μm. The two round capillary tubes are inserted in the square tube from opposite directions and three syringe needles are used to cover the inlets of the tubes. Epoxy is used to bond the syringe needles and seal the device to a glass slide.

Microencapsulated droplets are created by flowing three fluids synchronously in the device: (1) precursors of HKUST-1 (inner fluid), (2) a hydrophobic UV photopolymerizable silicone (shell fluid) (TEGO RAD 2650, EVONIK, Parsippany, NJ) as the shell material and (3) an aqueous surfactant-containing carrier fluid (outer fluid). The precursor solution of HKUST-1 is prepared by dissolving Cu(NO<sub>3</sub>)<sub>2</sub>·H<sub>2</sub>O and 1,3,5-benzene tricarboxylic acid (H<sub>3</sub>BTC) into N,N-dimethylformamide (DMF) with the molar ratio of Cu(NO<sub>3</sub>)<sub>2</sub>·H<sub>2</sub>O/H<sub>3</sub>BTC/DMF to be 3/2/67. Cu(NO<sub>3</sub>)<sub>2</sub>·H<sub>2</sub>O and H<sub>3</sub>BTC are separately dissolved in DMF and stirred for 1 h to ensure complete dissolution of the organic ligand and the metallic salt. In order to prevent any salt precipitation prior to the encapsulation, the two solutions are mixed right before each experiment. The outer carrier fluid consists of 40 wt% of glycerol (>99%) and 60 wt% of 1 wt% poly(vinyl alcohol) (PVA) aqueous solution. Unless otherwise stated, all chemicals were purchased from Sigma Aldrich and used as received.

The inner, shell, and outer fluid are continuously fed into the junction of the microchannel using three syringe pumps (NE-1010, New Era Pump System Inc., Farmingdale, NY) at a flow rate from 200 to 5000 μL h<sup>-1</sup>. The co-flow of the inner and the shell fluid is pinched off by the drag force of the outer fluid. Once the double droplets are formed, they are quickly cured for 10 s under UV light with 302 nm wavelength (Pierce

3UV Lamp, Thermo Fisher Scientific) to form the solid shell. Next, the obtained microcapsules containing MOF precursor solutions are heated to 90 °C and an isothermal reaction is carried out while visually monitoring the HKUST-1 synthesis. After 60 min, microcapsules now containing HKUST-1 crystals are collected in a glass vial and submerged in an ice bath to avoid any further crystallization. The images of microcapsules are taken by an optical microscope (B120C-E1, AmScope Inc., Irvine, CA). The MOF-bearing microcapsules are washed with ethanol and water alternatively three times and then vacuum dried at 180 °C for 24 h.

HKUST-1 is also synthesized via the conventional method, by reacting the bulk precursor solution at 90 °C for 24 h. The product is separated from the solvent via filtration and washed using ethanol and water alternatively three times. The sample is heated at 180 °C for 12 h and preserved in a drying cabinet.

## 2.2. Characterization of HKUST-1 and in-capsule synthesized HKUST-1

In order to analyze encapsulated HKUST-1, hexane is used to dissolve the shell material by leaving it overnight. Once MOFs are separated, they are washed with ethanol and water alternatively three times. The washed HKUST-1 particles are heated up to 180 °C for 12 h following the same preparation method as the conventionally prepared HKUST-1.

The microtomography technique at 13-BMD Advanced Photon Source (APS), Argonne National Laboratory (ANL), is used to identify the size and the location of MOFs within the capsules. The microtomography scans are obtained and the data are processed to reconstruct 3D images of the sample. The encapsulated MOFs sample is loaded in a 2 mm I.D. and 2.4 mm O.D. glass tube, and the glass tube is placed in the rotating sample holder. During the measurement, an X-ray beam (33.269 keV) impinges the rotating glass tube containing encapsulated MOFs particles and the X-ray intensity attenuations for multiple beam paths are measured by a detector. The resolution of the obtained microtomography images is 1.43  $\mu\text{m}/\text{pixel}$ . The morphology of HKUST-1 and encapsulated HKUST-1 is unveiled by using a Zeiss Sigma VP Scanning Electron Microscope (SEM). The samples are first gold coated and SEM images are generated by scanning a focused beam of high-energy (5 kV) electrons across the sample.

Thermogravimetric analysis (TGA) (LabSys Evo, Setaram) is used to investigate the thermal stability of neat MOFs and MOF-bearing microcapsules. Around 50 mg of the sample is placed in the crucible and heated up at the rate of 5 K  $\text{min}^{-1}$  from room temperature to 800 °C in  $\text{N}_2$  atmosphere. For encapsulated HKUST-1, The temperature is first increased to 180 °C and is maintained for 2 h, and then increased to 800 °C. The residue collected from the TGA experiments is used to measure the copper content in each capsule. 0.1 g of residue which is collected from multiple TGA experiments is dissolved in 10 mL of 10%  $\text{HNO}_3$  solution with sonication to

ensure complete leaching of copper. After dissolution, the copper solution is diluted by 20-fold and analyzed using the Inductively Coupled Plasma Atomic Emission Spectroscopy (ICP-AES) to determine the copper concentration.

A Malvern Panalytical XPert3 Powder X-Ray Diffraction (XRD) platform is employed to verify whether the MOFs directly synthesized within capsules are in fact HKUST-1. For phase identification of the encapsulated MOF, X-ray diffraction was performed with a Cu source, PIXcel1d detector. The sample was dispersed on a silicon zero-background wafer and rotated during the scan at 0.25 Hz. Data was collected from 5 to 50° (2 $\theta$ ) with a resolution of 0.0016°/step and a scanning rate of 0.5°  $\text{min}^{-1}$ . Thus, the total sampling time is roughly 1.5 h.

## 2.3. CO<sub>2</sub> capture experiments

The TGA setup (LabSys Evo, Setaram) is employed to investigate the CO<sub>2</sub> capture performance of the encapsulated HKUST-1 at 40 °C and atmospheric pressure. Ten cycles of CO<sub>2</sub> adsorption and desorption are carried out, where pure CO<sub>2</sub> is used for the CO<sub>2</sub> adsorption step and pure N<sub>2</sub> is used for the CO<sub>2</sub> desorption step. In every cycle, the mass change of the sample is recorded and the amount of CO<sub>2</sub> captured per gram of HKUST-1 is subsequently calculated.

## 3. Results and discussion

### 3.1. Microcapsule design and fabrication

Our encapsulated MOF is produced using a double-capillary device similar to the one developed by Vericella et al. at Lawrence Livermore National Laboratory [21]. The microfluidic device consists of nested capillary tubes with three inlets fed by different fluids. The inner fluid (CO<sub>2</sub> capture solvent with high viscosity in previous designs), the shell fluid, and the outer fluid (the carrier media consisting of an aqueous glycerol and surfactant solution) are pumped into the microfluidic device at controlled flow rates [30,31]. The shell material is a photopolymerizable silicone, which polymerizes under the exposure of ultraviolet (UV) light.

In this study, a mixture of MOF precursor solutions is used as the inner fluid and a heating system is integrated downstream of the UV-curing zone for the in-capsule synthesis of MOFs. As shown in Fig. 1, double emulsion droplets of the MOF precursor solutions and the shell fluid are produced and subsequently cured by UV light to generate microcapsules. The microcapsules are then heated up to 90 °C for 1–15 min to crystallize the MOFs in-situ. In order to activate the MOFs, the solvent inside the capsules is removed at 180 °C and the final product is in the form of micro-size particles of MOFs confined in a hollow shell. As shown in Fig. 2(a), the microcapsules are highly uniform in geometry and size. The average capsule diameter is between 300 and 500  $\mu\text{m}$  and the shell thickness is about 35–75  $\mu\text{m}$  depending on the system

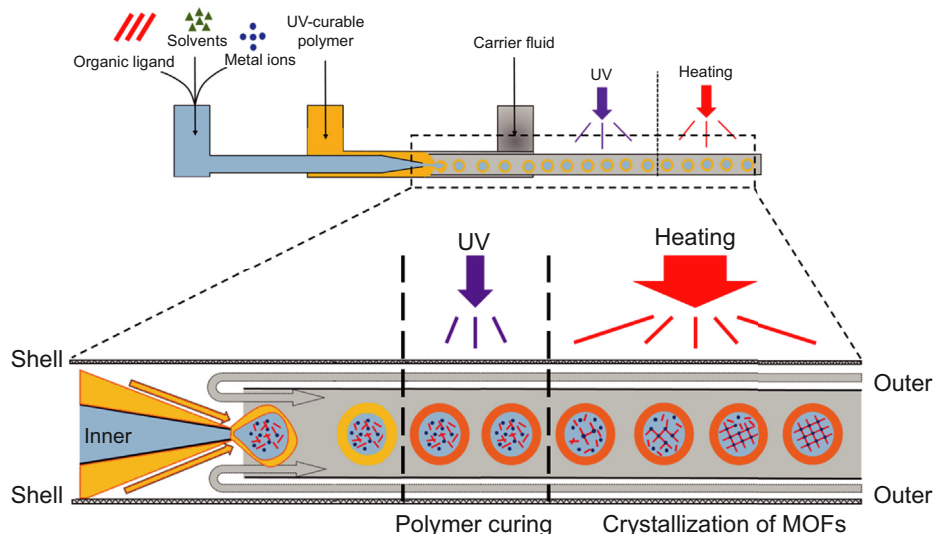


Fig. 1. Schematic of the microfluidic system for in-situ encapsulated synthesis of MOFs. The structure of the shell material, TEGO Rad 2650, is similar to that of TEGO Rad 2100 and TEGO Rad 2500 [32].

dimensions of the microfluidic device as well as the properties of fluids (e.g., the viscosity of the carrier media). Our previous studies have also shown that the size of microcapsules can be tuned by altering the flow rates of the three fluids [19].

HKUST-1 is selected as the first MOF to be synthesized via the microencapsulation method since it is well-studied for  $\text{CO}_2$  capture for its selectivity in the capture of  $\text{CO}_2$  from a gas mixture [33]. Further, its mild synthesis conditions (i.e.,  $90^\circ\text{C}$ , ambient pressure) and slow crystallization kinetics make it ideal for visual observation of MOF crystal formation inside of the capsules. The precursor solution of HKUST-1 is generally prepared by dissolving  $\text{Cu}(\text{NO}_3)_2 \cdot \text{H}_2\text{O}$  and  $\text{H}_3\text{BTC}$  to a homogeneous solution of DMF, Ethanol (EtOH), and deionized water ( $\text{H}_2\text{O}$ ) [29,33,34]. Unfortunately, ethanol and water can easily permeate through the UV-cured shell material, leading to the potential precipitation of precursor salts before the

heated reaction step. Thus, the method is modified by removing ethanol and water and the mass ratio of  $\text{Cu}(\text{NO}_3)_2 \cdot \text{H}_2\text{O}$  and  $\text{H}_3\text{BTC}$  is proportionally increased to ensure a high yield of MOF.

### 3.2. In-situ synthesis of MOFs within the encapsulated system and their visualization

One of the proposed benefits of our novel in-capsule synthesis of MOFs is the significant reduction of the synthesis time. The conventional ways of MOF synthesis via hydrothermal or solvothermal reactions are often time-consuming, and thus, MOF crystallization and the formation of the porous network can take several hours to days [35]. A recent study has shown that a micro-chemical process performed using droplets can significantly reduce the time required for MOFs

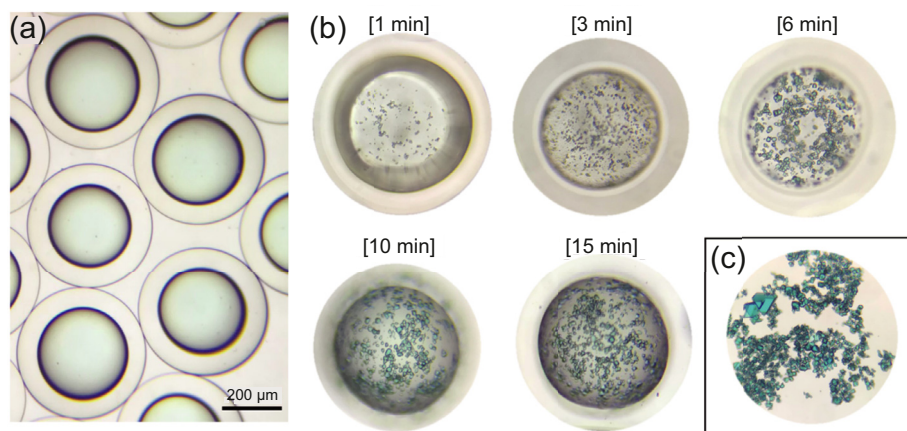


Fig. 2. Microscopic photos of encapsulated HKUST-1. (a) Produced microcapsules containing HKUST-1 precursor solutions (i.e.,  $\text{Cu}(\text{NO}_3)_2 \cdot \text{H}_2\text{O}$  and  $\text{H}_3\text{BTC}$  dissolved in a homogeneous solution of DMF prior to heating); (b) The stages of HKUST-1 crystal formation during the in-situ thermal reaction within the microcapsules (reaction time: 1–15 min); (c) Image of HKUST-1 crystals synthesized via the conventional solvothermal method using a bulk solution given as a comparison.

synthesis [29]. A number of MOFs (e.g., HKUST-1, MOF-5, IRMOF-3, and UiO-66 – not specific for CO<sub>2</sub> capture) have been successfully synthesized by creating micro-droplets containing metallic salts and organic Ligands dissolved in a polar medium [29]. For example, the synthesis time of HKUST-1 is reduced from two weeks to as short as 12 min [29]. Once synthesized, MOFs are separated, washed using ethanol, and dried. While this study demonstrated a significant reduction in MOF synthesis time, the final product is still a fine MOF powder, which would require further processing before its application for gas separation.

In order to monitor the formation Kinetics of HKUST-1 in our capsules, the reaction is carried out under a microscope. As can be observed from Fig. 2(b), during the entire synthesis period the capsule maintains its uniform size. HKUST-1 crystals become clearly visible after just 1 min of heated reaction. The reaction is completed in the first 10 min of heating, indicating a fast HKUST-1 formation rate similar to the study by Faustini et al. [29] The HKUST-1 crystals inside of the capsules have polyhedral shapes similar to MOFs synthesized via a conventional solvothermal method (Fig. 2(c)). Since heat and mass transfer is enhanced by the high surface area to volume ratio of the confined environment, fast crystallization of MOFs is achieved in the droplets. Further, the shell material effectively confines the MOF precursors inside, and therefore, HKUST-1 is only formed inside the capsules and simultaneously packaged for its deployment in various reactor systems.

It is hard to distinguish the distribution of the MOF crystals in three dimensions with a two-dimensional image (Fig. 2). Thus, microtomographic images of encapsulated MOF sorbents were taken at Argonne National Laboratory to identify

the precise location of the MOF crystals within the capsules and determine whether they are agglomerated into larger clusters. Two types of microcapsules, as made and dried capsules, are characterized and their 3-D tomographic images are shown in Fig. 3. HKUST-1 crystals are characterized by the bright part of the image. It is clear that the majority of HKUST-1 crystals are adherent to the inner surface of the capsules, meanwhile, some of them are embedded in the shell membrane. This pattern of the distribution of MOF crystals would allow the shortest mass transfer distance once CO<sub>2</sub> diffuses through the shell membrane, leading to a fast CO<sub>2</sub> capture rate. The tomographic images of dried and activated HKUST-1 microcapsules show a dense packing of MOF crystals that are well packed within the gas permeable shell. Overall, the dried capsules appear to take the shape of buckled spheres, which would alter the packing and transport behaviors in gas sorption processes.

### 3.3. Characterization of MOFs

In order to confirm that these crystals observed within the capsules are in fact HKUST-1, a series of characterization tools are used and crystals collected from microcapsules are compared to HKUST-1 prepared via a conventional synthesis method. As shown in Fig. 4(a) and (b), the HKUST-1 octahedral crystals found inside microcapsules are in the range of 0.5–7 μm, which is similar to HKUST-1 reported in the literature [29]. A few larger crystals are also observed in some cases. The SEM image (Fig. 4(a)) verifies the location of MOF crystals adhered to the inner wall of the shell membrane, which agrees with the findings from the microtomography images (See Fig. 3). The XRD patterns shown in Fig. 4(c)

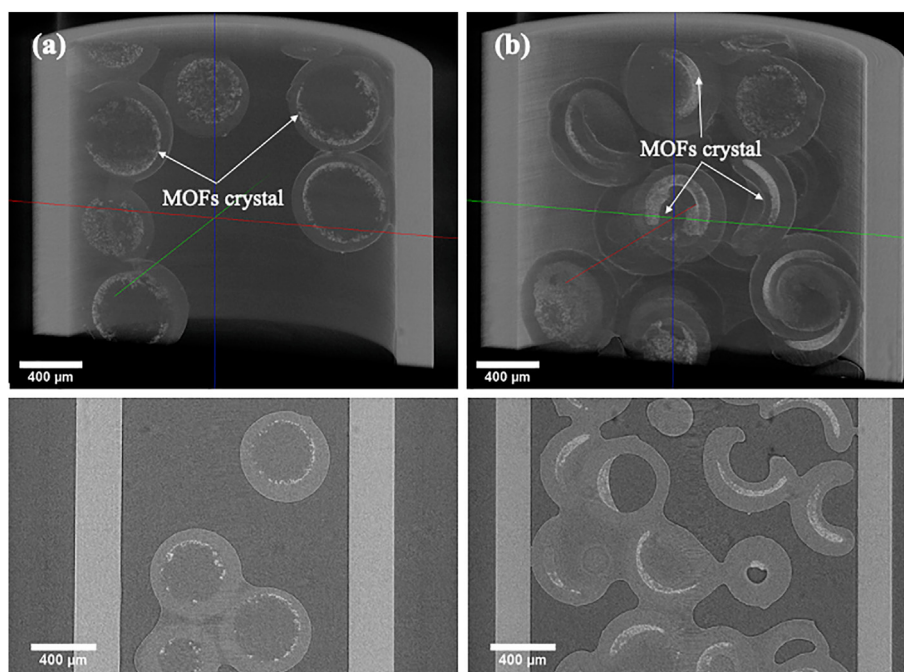


Fig. 3. 3-D X-ray microtomography of encapsulated HKUST-1 in a glass tube. (a) Microcapsules containing HKUST-1 and the remaining DMF solvent; (b) Dried microcapsules after removing the solvent.

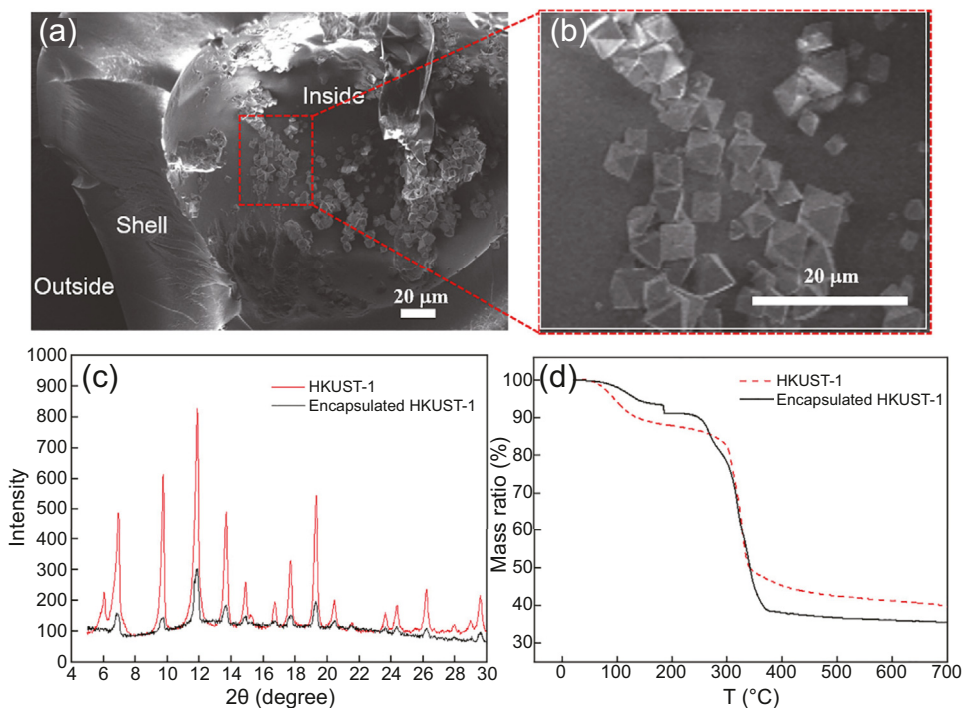


Fig. 4. (a) SEM image of the cross-section of a microcapsule loaded with HKUST-1; (b) SEM image of HKUST-1 particles found inside the microcapsules; (c) XRD spectra of HKUST-1 synthesized via an in-capsule synthesis method and a conventional solvothermal method; (d) Thermal decomposition behavior of neat HKUST-1 and microcapsules bearing HKUST-1.

confirm that the crystals obtained via the in-capsule synthesis approach have an identical crystal structure of HKUST-1 synthesized by the conventional solvothermal method (red spectra) [36]. The specific surface area and total pore volume of HKUST-1 were found to be  $2185 \text{ m}^2 \text{ g}^{-1}$  and  $0.57 \text{ cm}^3 \text{ g}^{-1}$ , respectively, which is comparable to other values previously reported in the literature [37,38].

The TGA curve of encapsulated HKUST-1 (red solid line) given in Fig. 4(d) shows a similar trend as that of the neat HKUST-1 crystals (black solid line), both exhibiting an initial stage of a small mass loss followed by a plateau, and a final stage of sharp weight loss. Compared to neat HKUST-1, there is a mass decrease of about 10 wt% when the temperature was maintained at  $180 \text{ }^\circ\text{C}$  for encapsulated HKUST-1, which was due to the evaporation of the solvent (DMF) trapped in the micro-pores of the crystals. This mass reduction would not be observed if the polymeric shell is not permeable for the solvent molecules (DMF). It is important not only to synthesize MOFs but also to fully remove the solvent so that the pores in MOFs are activated to capture  $\text{CO}_2$ . The encapsulated MOFs remain thermally stable until  $280 \text{ }^\circ\text{C}$ , followed by a sharp decrease in mass due to the thermal decomposition of the shell and MOFs. Finally, about 35 wt% of the residue is left, which should be the silicon oxide (from the shell) and copper oxide (from the HKUST-1). The TGA peaks associated with the neat HKUST-1 are in accordance with the literature [34].

Finally, in order to accurately quantify the HKUST-1 loading in each microcapsule, the residue from the TGA

experiment is dissolved and the copper content in the residue is determined using the ICP. The result shows a content of 1.64 wt% copper in the residue. Hence, the mass percentage of MOFs in each capsule is estimated to be 1.83 wt%. This low mass fraction of MOFs is attributable to the low concentration of precursor salts in precursor solutions which is limited by the optimal stoichiometric number. The loading of HKUST-1 in the microcapsules may be further increased if different solvents are used to dissolve HKUST-1 precursor salts at higher

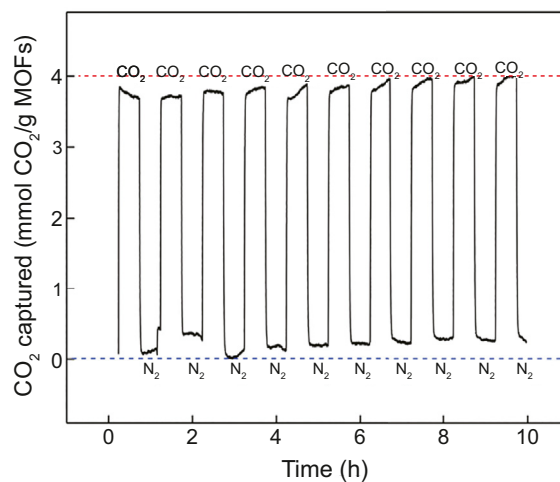


Fig. 5. Cyclic study of  $\text{CO}_2$  capture by encapsulated HKUST-1.

concentrations or by optimizing the shell layer towards a smaller thickness.

### 3.4. CO<sub>2</sub> capture using encapsulated MOFs

The CO<sub>2</sub> capture behavior of encapsulated HKUST-1 is investigated via a TGA analysis. The microcapsules are first heated up to 180 °C for 12 h to ensure the removal of all the solvents and activate HKUST-1. Ten cycles of CO<sub>2</sub> adsorption and desorption processes are carried out at 40 °C (typical CO<sub>2</sub> capture temperature at power plants) and atmospheric pressure using a CO<sub>2</sub>/N<sub>2</sub> swing. Fig. 5 shows the weight gain of the samples as CO<sub>2</sub> is absorbed and weight loss as CO<sub>2</sub> is removed with N<sub>2</sub>. The encapsulated HKUST-1 demonstrates rapid CO<sub>2</sub> adsorption and desorption rates, which very quickly reach equilibrium after switching to CO<sub>2</sub>. The pore size of the TEGO Rad layer was estimated to be 0.44 nm (D3) and 0.80 nm (D4) based on our Positron Annihilation Lifetime Spectroscopy (PALS) analysis, and its CO<sub>2</sub> permeability has been reported to be 3250 Barrer [39]. This suggests that the mass transfer resistance through the shell layer is minimal.

The CO<sub>2</sub> capture capacity is measured to be 4.0 mmol g<sup>-1</sup> - HKUST-1. This value is lower than the literature values, which is around 7.3 mmol g<sup>-1</sup> - HKUST-1 [33,34]. This may be due to a number of factors: defects in HKUST-1 crystals, incomplete activation of HKUST-1 and/or the interaction between HKUST-1 and the shell material. There is no strong experimental evidence aiming at a specific cause and the investigation is ongoing. After 10 cycles, the capture capacity is maintained, demonstrating the excellent recyclability and stability of the MOF-bearing capsules.

The overall CO<sub>2</sub> sorption and desorption processes by encapsulated MOFs are depicted in Fig. 6. First, CO<sub>2</sub> in the bulk gas phase is transferred through the gas-permeable polymer shell. The shell, on one hand, confines the MOF particles inside the microcapsules and on the other hand, protects the MOFs from the negative influences of moisture. Water vapor could lead to a decrease in the CO<sub>2</sub> capture

capacity and the damage of the MOFs structure due to an irreversible hydrolysis reaction [40], particularly for CO<sub>2</sub> capture from a power plant flue gas containing 4–6 vol% water [41]. The size and the thickness of the capsule shell would also impact the mass transfer behaviors of CO<sub>2</sub> and any other gases that are in the bulk phase. A thinner shell layer leads to lower mass transfer resistance but results in weaker mechanical strength of the sorbents. Additionally, the chemistry of the shell material could also significantly impact the selectivity of the overall CO<sub>2</sub> capture process.

The selection of MOFs that possess a high CO<sub>2</sub> capture capacity and selectivity is the first and most important step of the development of novel encapsulated MOF sorbents for rapid and efficient CO<sub>2</sub> capture. The mass transfer through the shell layer would be influenced by the CO<sub>2</sub> capture capacity and selectivity of MOF crystals confined in the polymer shell. The MOF-bearing microcapsule sorbents can be regenerated via a pressure swing as illustrated in this study, a temperature swing or both. Compared to fine HKUST-1 crystal powder (50 nm–20 μm) synthesized via a conventional method, handling MOF-bearing microbeads (300–500 μm) is significantly easier and safer. Furthermore, encapsulated MOFs can be applied in a wide range of reactor configurations including a fixed bed, a bubbling bed, or a fluidized bed reactor.

## 4. Conclusions

This is the first study showing the in-situ synthesis of MOFs directly within a polymeric shell. The MOF-bearing microcapsules is a new class of solid CO<sub>2</sub> capture sorbents that are mechanically robust, chemically stable, and environmentally benign. Our encapsulation scheme enables the use of microparticles of MOFs with a faster synthesis rate and a more flexible reactor application compared to fine powders of MOFs synthesized via a conventional mode. One of the most studied MOFs, HKUST-1, is selected as the first demonstration of this innovative approach. In-capsule synthesized HKUST-1 shows identical chemical properties as the MOFs prepared by the conventional solvothermal method. HKUST-1 microcapsules exhibit a fast CO<sub>2</sub> capture rate as well as high CO<sub>2</sub> capture capacity. The silicone shell did not slow down the CO<sub>2</sub> mass transfer and the HKUST-1 microcapsules show good recyclability and stability during multiple cycles of CO<sub>2</sub> capture and sorbent regeneration.

This first demonstration of the encapsulated synthesis of MOFs is important and opens a new area of research on hybrid sorbents with controlled mass transfer steps. A broader range of MOFs, such as MOF-5, UiO-66, IRMOF-3, Ru<sub>3</sub>BTC<sub>2</sub>, and Co<sub>3</sub>BTC<sub>2</sub> [29], can be readily explored using this facile approach to achieve faster synthesis and easy delivery for various applications. However, the synthesis of encapsulated MOFs is challenged by the low MOFs loading in the microcapsules due to a low concentration of the active components in the precursor solution, which could be improved by substituting the solvent for one with a higher solubility of the precursor salts or the optimization of shell thickness or employing other encapsulation techniques such as solvent

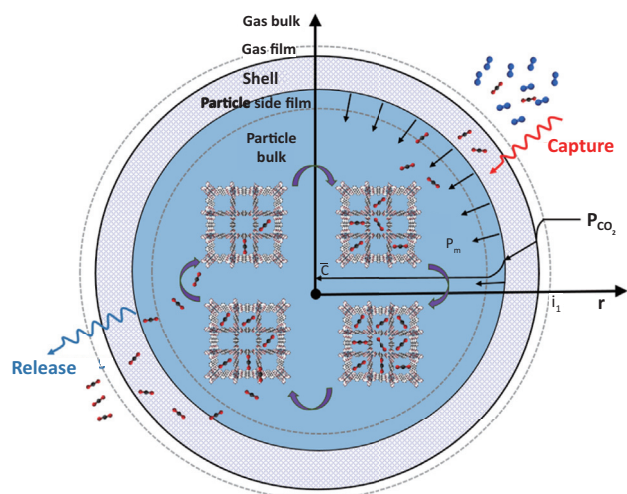


Fig. 6. Overall CO<sub>2</sub> sorption and desorption steps by encapsulated MOFs.

impregnated polymers (SIPs) [42]. Further, the mass production of such encapsulated materials needs to be considered for large-scale point source CO<sub>2</sub> capture or direct air capture. This would require a development of new techniques beyond microfluidic encapsulations such as solvent impregnated polymers (SIPs) [42]. The future development of the encapsulated MOFs can draw on extensive research on carbon capture sorbents (e.g., MOFs) and gas separation membranes.

### Declaration of competing interest

There is no conflict of interest.

### Acknowledgments

The authors acknowledge National Science Foundation (CBET 1927336), Saudi Aramco, and the Lenfest Center for Sustainable Energy at the Earth Institute at Columbia University for financially supporting this work. The microtomography of encapsulated MOFs was performed at GeoSoilEnviroCARS (The University of Chicago, Sector 13), Advanced Photon Source (APS), Argonne National Laboratory. GeoSoilEnviroCARS is supported by the National Science Foundation - Earth Sciences (EAR - 1634415) and the Department of Energy- GeoSciences (DE-FG02-94ER14466). This research used resources of the Advanced Photon Source, a U.S. Department of Energy (DOE) Office of Science User Facility operated for the DOE Office of Science by Argonne National Laboratory under Contract No. DE-AC02-06CH11357.

### References

- [1] D.J. Heldebrant, P.K. Koech, V.-A. Glezakou, R. Rousseau, D. Malhotra, D.C. Cantu, *Chem. Rev.* 117 (2017) 9594–9624.
- [2] E. and M. National Academies of Sciences, *Negative Emissions Technologies and Reliable Sequestration*, National Academies Press, Washington, D.C., 2018.
- [3] E. and M. National Academies of Sciences, *Gaseous Carbon Waste Streams Utilization*, National Academies Press, Washington, D.C., 2018.
- [4] T. Niass, Jordan Kislear, M. Buchanan, J. Svalestuen, A.-H.A. Park, D. DePaolo, J. Powell, *Accelerating Breakthrough Innovation in Carbon Capture, Utilization, and Storage*, Department of Energy, 2017.
- [5] W. Yu, T. Wang, A.H.A. Park, M. Fang, *Nanoscale* 11 (2019) 17137–17156.
- [6] G.T. Rochelle, *Science* 325 (2009) 1652–1654.
- [7] A. Samanta, A. Zhao, G.K.H. Shimizu, P. Sarkar, R. Gupta, *Ind. Eng. Chem. Res.* 51 (2012) 1438–1463.
- [8] Q. Wang, J. Luo, Z. Zhong, A. Borgna, *Energy Environ. Sci.* 4 (2011) 42–55.
- [9] H. Yu, X. Wang, Z. Shu, M. Fujii, C. Song, *Front. Chem. Sci. Eng.* 12 (2018) 83–93.
- [10] P.M. Bhatt, Y. Belmabkhout, A. Cadiau, K. Adil, O. Shekha, A. Shkurenko, L.J. Barbour, M. Eddaoudi, *J. Am. Chem. Soc.* 138 (2016) 9301–9307.
- [11] A.C. Forse, P.J. Milner, J.-H. Lee, H.N. Redfearn, J. Oktawiec, R.L. Siegelman, J.D. Martell, B. Dinakar, L.B. Porter-Zasada, M.I. Gonzalez, J.B. Neaton, J.R. Long, J.A. Reimer, *J. Am. Chem. Soc.* 140 (2018) 18016–18031.
- [12] A. Gładysiak, K.S. Deeg, I. Dovgaliuk, A. Chidambaram, K. Ordiz, P.G. Boyd, S.M. Moosavi, D. Ongari, J.A.R. Navarro, B. Smit, K.C. Stylianou, *ACS Appl. Mater. Interfaces* 10 (2018) 36144–36156.
- [13] F. Schüth, W. Schmidt, *Adv. Mater.* 14 (2002) 629–638.
- [14] G. Maurin, C. Serre, A. Cooper, G. Férey, *Chem. Soc. Rev.* 46 (2017) 3104–3107.
- [15] H.-C. Joe Zhou, S. Kitagawa, *Chem. Soc. Rev.* 43 (2014) 5415–5418.
- [16] A. Torrisi, R.G. Bell, C. Mellot-Draznieks, *Cryst. Growth Des.* 10 (2010) 2839–2841.
- [17] J. Yu, L.-H. Xie, J.-R. Li, Y. Ma, J.M. Seminario, P.B. Balbuena, *Chem. Rev.* 117 (2017) 9674–9754.
- [18] B. Valizadeh, T.N. Nguyen, K.C. Stylianou, *Polyhedron* 145 (2018) 1–15.
- [19] W. Yu, M. Gao, A.-H.A. Park, In: *Abstr. Pap. Am. Chem. Soc.*, 16TH ST, NW, WASHINGTON, DC 20036, AMER CHEMICAL SOC, USA, 256 (2018) 1155.
- [20] W. Yu, T. Wang, A.-H. Alissa Park, M. Fang, *Ind. Eng. Chem. Res.* 59 (2020) 9746–9759.
- [21] J.J. Vericella, S.E. Baker, J.K. Stolaroff, E.B. Duoss, J.O. Hardin, J. Lewicki, E. Glogowski, W.C. Floyd, C.A. Valdez, W.L. Smith, J.H. Satcher, W.L. Bourcier, C.M. Spadaccini, J.A. Lewis, R.D. Aines, *Nat. Commun.* 6 (2015) 6124.
- [22] J.K. Stolaroff, C. Ye, J.S. Oakdale, S.E. Baker, W.L. Smith, D.T. Nguyen, C.M. Spadaccini, R.D. Aines, *Faraday Discuss* 192 (2016) 271–281.
- [23] S.A. Nabavi, G.T. Vladislavjević, S. Gu, V. Manović, *Langmuir* 32 (2016) 9826–9835.
- [24] A. Raksajati, M.T. Ho, D.E. Wiley, *Ind. Eng. Chem. Res.* 56 (2017) 1604–1620.
- [25] J.R. Finn, J.E. Galvin, *Int. J. Greenh. Gas Control* 74 (2018) 191–205.
- [26] J.K. Stolaroff, C. Ye, D.T. Nguyen, J. Oakdale, J.M. Knipe, S.E. Baker, *Energy Procedia* 114 (2017) 860–865.
- [27] T. Moore, K.A. Mumford, G.W. Stevens, P.A. Webley, *AIChE J.* 64 (2018) 4066–4079.
- [28] K. Hornbostel, D. Nguyen, W. Bourcier, J. Knipe, M. Worthington, S. Mccooy, J. Stolaroff, *Appl. Energy* 235 (2019) 1192–1204.
- [29] M. Faustini, J. Kim, G.-Y. Jeong, J.Y. Kim, H.R. Moon, W.-S. Ahn, D.-P. Kim, *J. Am. Chem. Soc.* 135 (2013) 14619–14626.
- [30] S.A. Nabavi, T. Vladislavjević, V. Manović, M. Manović, *Chem. Eng. J.* 322 (2017) 140–148.
- [31] S.A. Nabavi, G.T. Vladislavjević, M.V. Bandulasena, O. Arjmandi-Tash, V. Manović, M. Manović, *J. Colloid Interface Sci.* 505 (2017) 315–324.
- [32] J. Pokorny, Richard, P. Thomas, *Hardcoats*, WO 2009/029438 A1, 2008.
- [33] S. Ye, X. Jiang, L.W. Ruan, B. Liu, Y.M. Wang, J.F. Zhu, L.G. Qiu, *Microporous Mesoporous Mater.* 179 (2013) 191–197.
- [34] X. Yan, S. Komarneni, Z. Zhang, Z. Yan, *Microporous Mesoporous Mater.* 183 (2014) 69–73.
- [35] C. Dey, T. Kundu, B.P. Biswal, A. Mallick, R. Banerjee, *IUCr, Acta Crystallogr. Sect. B Struct. Sci. Cryst. Eng. Mater.* 70 (2014) 3–10.
- [36] A. Sachse, R. Ameloot, B. Coq, F. Fajula, B. Coasne, D. De Vos, A. Galarneau, *Chem. Commun.* 48 (2012) 4749–4751.
- [37] S.M. Moosavi, A. Chidambaram, L. Talirz, M. Haranczyk, K.C. Stylianou, B. Smit, *Nat. Commun.* 10 (2019) 539.
- [38] Düren Tina, Millange Franck, Férey Gérard, Krista S. Walton, R.Q. Snurr, *J. Phys. Chem. C* 111 (2007) 15350–15356.
- [39] J.M. Knipe, K.P. Chavez, K.M. Hornbostel, M.A. Worthington, D.T. Nguyen, C. Ye, W.L. Bourcier, S.E. Baker, J.F. Brennecke, J.K. Stolaroff, *Environ. Sci. Technol.* 53 (2019) 2926–2936.
- [40] Y. Chen, Z. Qiao, J. Huang, H. Wu, J. Xiao, Q. Xia, H. Xi, J. Hu, J. Zhou, Z. Li, *ACS Appl. Mater. Interfaces* 10 (2018) 38638–38647.
- [41] H.A. Patel, J. Byun, C.T. Yavuz, *ChemSusChem* 10 (2017) 1303–1317.
- [42] G. Rim, T.G. Feric, T. Moore, A.-H.K. Park, *Adv. Funct. Mater.* 31 (2021) 2010047.